

Yap control of tissue growth relies on cell density and F-actin in zebrafish fin regeneration

Rita Mateus¹, Raquel Lourenço¹, Yi Fang², Gonçalo Brito³, Ana Farinho^{1,3}, Fábio Valério¹ and Antonio Jacinto^{1,4,*}

¹CEDOC, NOVA Medical School, NOVA University of Lisbon, Campo Mártires da Pátria 130, 1169-056 Lisboa, Portugal

²National Institute of Environmental Health Sciences, Research Triangle Park, North Carolina, 27709 United States

³Instituto de Medicina Molecular, Faculdade de Medicina, Universidade de Lisboa, 1649-028 Lisboa, Portugal

⁴Instituto Gulbenkian Ciência, Rua da Quinta Grande 6, 2780-156 Oeiras, Portugal

* Corresponding author: Antonio Jacinto – antonio.jacinto@fcm.unl.pt

(+351) 214464548 ext.548

Summary

Caudal fin regeneration is characterized by a proliferation boost in the mesenchymal blastema controlled precisely in time and space. This allows a gradual and robust restoration of original fin size. However, how this is established and regulated is not well understood. Here we report that Yap, the Hippo pathway effector, is a chief player in this process: functionally manipulating Yap during regeneration dramatically affects cell proliferation and expression of key signaling pathways, impacting regenerative growth. The intracellular location of Yap is tightly associated with different cell densities along the blastema proximal-distal axis, which correlate with alterations in cell morphology, cytoskeleton and cell-cell contacts in a gradient-like manner. Importantly, Yap inactivation occurs in high cell density areas, conditional to F-actin distribution and polymerization. We propose that Yap is essential for fin regeneration and its function is dependent on mechanical tension, conferred by a balancing act of cell density and cytoskeleton activity.

Keywords

Zebrafish, fin regeneration, Hippo/Yap, F-actin, cell density

Introduction

The ability of adult vertebrates to regenerate lost or injured organs is restricted to few examples in nature. The zebrafish (*Danio rerio*) is one of these impressive cases, being able to regrow a fully functional and anatomically similar organ through epimorphic regeneration (Morgan, 1901; Poss et al., 2000). In particular, caudal fin regeneration proceeds in three main phases: wound healing, blastema formation and outgrowth. Upon amputation, wound healing starts by immediate migration of the epidermis adjacent to the stump, which will give rise to a specialized wound epidermis (Poleo et al., 2001; Lee et al., 2009). The blastema will then begin to form, entailing the migration of differentiated intrarray mesenchymal cells towards the stump that de-differentiate and proliferate in a lineage restricted fashion (Knopf et al., 2011; Sousa et al., 2011; Stewart and Stankunas, 2012). Once the blastema is completely formed, it is divided into regions: a distal region associated with little proliferation and stem cell-like properties and a proximal region where most of the proliferation and differentiation events occur. Then in the outgrowth phase, these regions become more distinct, with a non-proliferative distal most blastema tip, a medial region where cell proliferation is mainly occurring and a proximal area where differentiation is taking place (Nechiporuk and Keating, 2002; Wehner et al., 2014).

Remarkably, upon amputation the caudal fin regenerates the precise amount of tissue that was lost, at the correct location. This indicates that a positional memory instructs the blastema cells according to their proximo-distal fin localization (Lee et al., 2005). Coupled to this property, the regenerative process occurs independently of the number of amputations applied and animal age (Azevedo et al., 2011). Such properties point toward a tight growth control program, involving precise coordination between proliferation and positional information along the regenerating caudal fin. Though it is yet unclear how these two central processes are molecularly controlled, they most likely comprise the integration of various signals. To date, FGF is the only morphogen that was shown to promote a proliferation rate increase in a proximal-distal gradient-like manner (Lee et al., 2005). Recently, the inhibition of the phosphatase Calcineurin and potassium channel activity were shown to be necessary for the fin proportionate growth

during development and regeneration (Perathoner et al., 2014; Kujawski et al., 2014). Clearly, further clarification of the cellular mechanisms that restrain uncontrolled proliferation is in order to understand what regulates the final size of the renewed organ.

One signaling pathway that has arisen as a candidate for growth control during regeneration is the conserved Hippo pathway, which is essential for proper regulation of developmental organ growth in *Drosophila* and vertebrates (Pan, 2010). This kinase cascade can be activated by multiple inputs and ultimately converges in phosphorylation and inactivation of its effectors, the transcriptional activator Yap and its paralogue Taz, by excluding one or both from the nucleus (Huang et al., 2005; Dong et al., 2007). In the nucleus, Yap/Taz bind to different partners, namely the TEAD family of transcription factors, together stimulating the transcription of multiple target genes (Mahoney et al., 2005; Zhao et al., 2008).

Different studies have implicated the Hippo pathway in repair mechanisms. Several reports have shown a role for this pathway as a mediator of intestinal and heart repair, as well as limb bud regeneration (Cai et al., 2010; Staley and Irvine, 2010; Hayashi et al., 2014). Moreover, the link between extracellular matrix (ECM) stiffness, cell morphology and the actin cytoskeleton has been proven as a mode for Yap/Taz activation *in vitro* (Dupont et al., 2011). Activation of Yap/Taz can also be cell density dependent (Zhao et al., 2007), possibly through the action of adherens junctions (Schlegelmilch et al., 2011). These findings demonstrate that cells are able to interpret physical signals from their surroundings through Yap/Taz, but transduction of mechanical cues into actual signaling is still little understood *in vivo*. Importantly, in zebrafish organ regeneration, including the caudal fin, where accurate growth must be controlled, this pathway has never been addressed. Furthermore, the study of mechanotransduction, cytoskeleton and adhesion has remained limited in this *in vivo* context (Santos-Ruiz et al., 2005).

Here we explore the hypothesis that changes in tissue tension and cell density, inherent to wounding and regeneration of the caudal fin, trigger a series of events that contribute to regeneration involving the Hippo pathway. Our results indicate that Yap is indispensable for proliferation in the blastema and necessary for regeneration to proceed. Interestingly, we found

that Yap inactivation correlates with high cell density areas and localization of Alpha-Catenin and F-actin. This suggests that tension changes, which result from heterogeneous cell densities and are sensed by the junctions and cytoskeleton, influence growth within the blastema. We propose the blastema tissue is constrained by mechanical forces that are mechanotransduced by Yap, contributing for final size recovery during epimorphic regeneration.

Results

Yap intracellular localization varies according to the stage and region of the blastema

A hallmark of Yap and Taz activation is their translocation from the cytoplasm to the nucleus (Yagi et al., 1999; Zhao et al., 2007; Oh and Irvine, 2008). To understand whether Yap is activated during the caudal fin regenerative process, we assessed its protein expression in longitudinal sections of fin rays by immunofluorescence. This characterization showed striking intracellular dynamics in several regeneration stages. At 6 hours post amputation (hpa), mesenchymal cells in the segment next to the amputation plane displayed Yap in the nucleus, contrasting to uncut and 3hpa fins, where Yap was uniformly present in the cytoplasm (Fig. 1A-C,G). This suggests that Yap becomes activated early in the regenerative process, during wound healing. The nuclear localization of Yap was maintained at 24hpa, as mesenchymal cells form the blastema (Fig. 1D). By 48hpa, when the blastema was complete, we detected different regions of intracellular Yap: in proximal regions Yap was mostly nuclear, whereas distally it was mainly cytoplasmic (Fig. 1E,G). This correlates with known proliferative regions in the blastema (Nechiporuk and Keating, 2002), where the proximal region contains most of the proliferative events in contrast with the distal region. Finally, during blastema outgrowth at 72hpa, these regions were more defined, with Yap more cytoplasmic in distal most regions and progressively becoming nuclear towards proximal regions (Fig. 1F,G). This led us to believe that Yap could be playing an active role in controlling proliferation during caudal fin regeneration. Of note, the average intensity ratios between nuclear and cytoplasmic Yap in 48hpa and 72hpa distal most regions were similar to uncut fin values, suggesting that Yap is inactive in these blastema areas (Fig. 1G).

To determine if other Hippo pathway members were present during zebrafish caudal fin regeneration, we analyzed their expression in different regenerative stages through *in situ* hybridization and quantitative PCR (qPCR) (Fig. S1A-B). The core components of the pathway (*stk3*, *sav1*, *lats2*, *yap1*, *wwtr1*, *nf2b*, *fird6*) and possible Yap DNA binding partners (*tead1a*

and *tead4*) were expressed in the blastema. However, Hippo pathway core components were not upregulated upon amputation, indicating that transcription does not play a key role in the pathway's regulation. Subsequently we addressed the expression of phosphorylated active forms of Mst1/2 and Lats1/2 as well as total NF2 in 72hpa blastemas by immunohistochemistry. We distinguished increased phosphorylated Mst1/2 and Lats1/2 in distal areas (Fig. S1C-D,F-G) and presence of NF2 throughout the blastema (Fig. S1E). This suggests that Hippo pathway components capable of inactivating Yap are active specifically in distal regions where Yap is mainly cytoplasmic. These results show that this pathway is conserved in zebrafish and activated in the blastema during caudal fin regeneration.

Yap controls proliferation levels during regeneration

To determine whether Yap controls proliferation during regeneration, we used heat-shock transgenics to functionally manipulate Yap. These allowed us to constitutively activate Yap (hsp70:RFP-CAyap, referred as CA-yap, Fig. S2A) and to dominantly inactivate Yap (hsp70:RFP-DNyap, referred as DN-yap, Fig. S2A). DN-yap transgenics were validated by addressing the previously demonstrated requirement of Yap for cardiac precursor cell migration, using morpholinos (Fig. S2B-M) (Fukui et al., 2014; Miesfeld and Link, 2014). Moreover by performing immunostainings against RFP and Yap in both transgenic lines, we observed co-localization (Fig. S3A-F).

Upon single heat-shock, *yap1* expression was induced 6-fold in CA-yap and 115-fold in DN-yap transgenics (Fig. 2B). In both cases, by applying a daily heat-shock during the blastema forming phases (24 and 48hpa, Fig. 2A), regeneration was impaired at 72hpa (Fig. 2C-F). To understand if the phenotypes could be due to proliferation defects, we applied the same protocol in functional Yap transgenics coupled to S/G2/M cell cycle marker transgenics, Eflα:mag-zGeminin (Sugiyama et al., 2009). Immunohistochemistry analysis of Geminin together with the mitosis marker phospho-Histone 3 (pH3), revealed more proliferation in CA-yap double transgenics resulting in deformed but smaller blastemas by 60hpa when compared to siblings

(Fig. 2G-H,L). In DN-yap transgenics, proliferation was reduced causing undersized blastemas. This likely happens due to cell cycle delay at G2/M phases (Xia et al., 2002), since cells were able to enter the cell cycle and express Geminin, but not proceed to mitosis, shown by the reduction of pH3 (Fig. 2I-J,M). To further understand the effects of Yap manipulation in proliferation, we performed single heat-shocks in 72hpa CA-yap transgenics injected with EdU, the S-phase cell cycle marker (Choi et al., 2013). Importantly, we detected a progressive increase in EdU positive cells in CA-yap positive blastemas by 6 hours post heat-shock (hpHS) and 12hpHS, but not in siblings or 3hpHS (Figs 2N-P, S4A-D). To address the small blastema phenotypes in both Yap transgenics we performed TUNEL, cell death analysis (Cole et al., 2001). Interestingly, there was also a gradual increase of cell death in CA-yap⁺, starting at 18hpHS, after the main proliferative hpHS (6 and 12hpHS). This did not occur in siblings or DN-yap⁺ transgenics, indicating that in the latter case, reduction in blastema size is likely due to less proliferation (Fig. S4E-N). Interestingly, the ectopic cell death is observed almost exclusively in the CA-yap⁺ epidermis, pointing towards a possible impairment of the wound epidermis (perhaps affecting its signaling function) consequently resulting in small blastema phenotypes in CA-Yap⁺ transgenics.

Additionally, we observed differences in Yap-RFP intracellular dynamics: in CA-yap, Yap-RFP is predominantly nuclear (Fig. 2H'-H'') while in DN-yap, Yap-RFP is more cytoplasmic (Fig. 2J'-J''). These observations were supported by quantifying the average intensity ratios between nuclear and cytoplasmic Yap-RFP, in both functional transgenics (Fig. 2K). Ratios in CA-yap⁺ transgenics were comparable to ratios found in areas of WT blastemas where Yap is mainly active, while DN-yap⁺ ratios showed similar values to the ones obtained in inactive Yap zones (compare Fig. 2K with Fig. 1G), confirming the intracellular localization of CA-Yap and DN-Yap proteins, since they functionally localize to the expected intracellular compartment. Together these results suggest that proliferation needs to be tightly regulated for regeneration to occur.

Yap regulates the expression of known targets and regeneration factors

To ascertain that manipulating Yap affects its activation state by inducing transcription of downstream genes, we searched for bona fide Yap transcriptional targets in the blastema by performing qPCR upon heat-shock induction in Yap functional transgenics. We found that *connective tissue growth factor A (ctgfa)* and *amphiregulin (areg)*, two of Yap's well characterized targets (Zhao et al., 2008; Zhang et al., 2009), were upregulated in CA-yap⁺ transgenics but not in DN-yap⁺ when compared to control siblings (Fig. 3A-B). Since in zebrafish *ctgf* is duplicated (Fernando et al., 2010), we confirmed the observed effect is *ctgfa* specific (Fig. S3G). Upregulation of *ctgfa* in response to Yap activation was also shown through *in situ* hybridization in CA-yap transgenics versus siblings, upon single heat-shock (Fig. S3H-I). In addition, we monitored *ctgfa* activation dynamics *in vivo* with a reporter line (*ctgfa:eGFP*, Fig. S2A) coupled to Yap transgenics. We observed that by 7hpHS, the expression of *ctgfa* was upregulated in 72hpa blastemas of double transgenics *ctgfa:eGFP*; CA-yap⁺ when compared to siblings (Fig. 3C-D,G). Conversely, in *ctgfa:eGFP*; DN-yap⁺ transgenics, *ctgfa* expression remained equal to controls, in agreement with qPCR results (Fig. 3E-F,H). Furthermore, evidence of Yap activation in double transgenics *ctgfa:eGFP*; CA-yap was obtained by performing immunofluorescence against Yap and GFP in the same fins monitored *in vivo* (Fig. S3J-M). We observed that at 7hpHS, Yap was more nuclear in those fins, confirming the heat-shock efficiency. These results allow concluding that the regeneration phenotypes observed in the functional transgenics are specific to Yap manipulation and that *ctgfa* is likely to be a direct target of Yap in zebrafish, as it is in higher vertebrates. Of note, *ctgf* can also be a transcriptional target of other pathways, namely WNT and TGF β (Luo et al., 2004; Fujii et al., 2012). This possibly explains GFP expression of the *ctgfa:eGFP* reporter, occurring even in mesenchymal regions where Yap is not active, indicating the existence of other means of *ctgfa* regulation not exclusive of Yap (Fig. S3J-K).

To further explore these observations, we analyzed the expression of several genes involved in regeneration by performing qPCR upon heat-shock in Yap transgenics. We found that in CA-

yap⁺ transgenics, a number of these factors were significantly downregulated, namely *fgf20a*, *wnt10a*, *lef1* and *shh*, while *dkk1b* was highly upregulated (Fig. 3I). In contrast, DN-yap⁺ transgenics presented the opposite tendency of expression, with *fgf20a* upregulated (Fig. 3J). Of interest *msxB*, *bmp2a* and *bmp2b* were unaltered upon Yap manipulations (Fig. 3I-J). This indicates that Yap has the ability to regulate a number of key regeneration factors. The regeneration impairment occurring in CA-yap and DN-yap transgenics is likely a combination of changes in expression of those factors and cell proliferation.

Yap does not affect *ctgfa* expression in uncut fins

Fins grow throughout the life of adult fish, depending on a homeostasis process involving some of the genes necessary for epimorphic regeneration (Wills et al., 2008). To test if in uninjured fins Yap could lead to proliferation phenotypes related to the ones observed during regeneration, we applied the same heat-shock protocol as before (Fig. 2A) to both Yap transgenics and siblings in uncut situations. Remarkably, in uncut fins CA-yap induction lead to no morphological changes (Fig. S5A-B). Also upregulation of *ctgfa* was not detected by 7hpHS in uncut double transgenics *ctgfa:eGFP*; CA-yap (Fig. S5C-D), indicating that CA-yap expression is not sufficient to stimulate the transcription of its target gene. This points toward the existence of a robust inhibitory mechanism for homeostatic proliferation in adult fins. The same results were observed in DN-yap uncut transgenics (Fig. S5E-H). Interestingly, applying the same single heat-shock protocol to *ctgfa:eGFP*; CA-yap double transgenics where only half of the caudal fin was amputated, *ctgfa* expression was upregulated by 7hpHS, in contrast to the uncut half fin (Fig. S5I-J).

The uninjured adult caudal fin tissue is known for its liability in silencing transgenes (Thummel et al., 2006). To confirm that the previous results were not consequences of such an effect, we applied single heat-shocks in Yap transgenics with 72hpa half fin amputations and performed *yap1 in situ* hybridizations. In both CA-yap⁺ and DN-yap⁺ there was a clear *yap1* upregulation upon transgene activation when compared to siblings expression (Fig. S5K-N), both in

amputated and uncut fins (Fig. S5K'-N',K''-N''). This indicates that Yap transgenes can be transcribed in uninjured, homeostatic situations, but fin cells appear to be in a non-responsive state. During epimorphic regeneration, however, cells appear to be prone to respond to Yap activity, causing specific phenotypes.

Cell density along the blastema associates with the localization of active Yap

One possible explanation for the regulation of Yap intracellular dynamics in the blastema is that changes in cell matrix rigidity and/or cell density triggered by the amputation can modify tissue tension, thus affecting cell morphology as well as cell area (Zhao et al., 2007; Dupont et al., 2011; Wada et al., 2011; Aragona et al., 2013). These changes could be sensed at the cell membrane, through its junctions and cytoskeleton, controlling Yap activation and proliferation levels (Schlegelmilch et al., 2011; Fernández et al., 2011). To test this hypothesis, we established a cell density map along the blastema proximal-distal (PD) axis by measuring the average intensity of mesenchymal nuclei in different regeneration stages. We found that at 24hpa, cell density was homogeneous along the PD axis (Fig. 4A,D). Strikingly, at 48 and 72hpa, when the blastema is complete, cell density was differential: higher in distal regions when compared to proximal regions of the same samples (Fig. 4B-C,E-F). The high cell density regions correlated with distal areas where Yap is mainly cytoplasmic, thus mostly inactive, suggesting that cell density could control Yap inactivation through *in vivo* contact inhibition of proliferation (compare Fig. 4E-F with Fig. 1E-F). To understand if these cell density changes translated into effects in cell morphology, we performed immunofluorescence against GFP in *ctgfa:eGFP* transgenics, as this marker labels all mesenchymal cells, in the same stages as before. We observed that at 24hpa, mesenchymal cells were variable in shape, presenting many protrusions, in agreement with their migratory phenotype during blastema formation (Fig. 4J,N). When quantifying the cell aspect ratio, which provides a measure of cell roundness (representing the relation among their *x* and *y* axes), we found that 24hpa mesenchymal cells were more elongated exhibiting an average aspect ratio of 0.42 (Fig. 4M). Moreover, by quantifying the

space between mesenchymal cells along the PD axis, we observed that 24hpa cells were uniformly spread throughout the blastema (Fig. 4G). At 48 and 72hpa, the distal mesenchymal cells became more compact (Fig. 4H-I,K-L,O-R), reflecting the density increase and not a major change in cell size along the PD axis. Regarding morphology, these distal cells showed significantly less variability in shape, being rounder and lacking protrusions (average aspect ratio of 0.71 and 0.67, for 48 and 72hpa respectively), when compared with cells of the corresponding proximal region (0.50 and 0.48, for 48 and 72hpa respectively) or 24hpa blastemas (Fig. 4M). This correlation between cell density and cell morphology along the blastema suggests that cells adapt their shape to tension changes and these mechanical cues might affect Yap activation.

Alpha-Catenin correlates with Yap intracellular localization

To find adhesion and cytoskeleton associated proteins that might act as cell density sensors in the blastema and mediators of Yap activation, we performed systematic immunohistochemistry in 48 and 72hpa blastemas searching for expression differences along the PD axis (Table S1). This led to the identification of several adhesion proteins present in specific cell types (Fig. S6). Interestingly, Alpha-Catenin was the only junctional protein localized in blastemas in a PD dependent manner. By performing immunostainings against Yap and GFP in Alpha-Catenin-Citrine protein trap transgenics (Žigman et al., 2010) at 72hpa, we observed that expression of endogenous Alpha-Catenin correlated with Yap intracellular dynamics (Fig. 5A-B). In particular, the junctional localization of Alpha-Catenin in the distal, dense and round mesenchymal cells corresponds to areas where Yap is more cytoplasmic (Fig. 5D,F,G-H Distal); conversely, in proximal areas where Yap is more nuclear and cells are sparse and protrusive, Alpha-Catenin was not present (Fig. 5C,E,G-H Proximal). Moreover, by quantifying intensity ratios between PD regions, we observed that 50% of Yap translocates from nucleus to cytoplasm. Interestingly, 50% of Alpha-Catenin changes intracellular location when comparing proximal to distal blastema regions (Fig. 6I). This suggests that Alpha-Catenin could constitute

an *in vivo* mechanosensor of cell density during regeneration, due to its apparent response to an increase in cell-cell contacts in the distal blastema, area that corresponds to Yap inactivation.

F-actin controls Yap activation

The cytoskeleton plays an active role in mediating mechanical forces to which cells are exposed, hence we investigated F-actin localization in the blastema. Phalloidin stainings showed F-actin also underwent changes along the PD axis in 72hpa blastemas (Fig. 6A-B): it localizes to the cortex in distal cells, where cell density is higher and Yap more cytoplasmic (Fig. 6C-D, G-H XZ Distal); while proximally, F-actin is present throughout the cell cytoplasm, in areas of lower density and nuclear Yap (Fig. 6E-F, G-H XZ Proximal). By quantifying F-actin and Yap proximal-distal intensity ratios, we observed that changes in F-actin intracellular location in PD regions were even greater than Yap's (Fig. 6I). F-actin also co-localized with junctional Alpha-Catenin in distal blastemas (Fig. S7A-F).

To determine whether F-actin is involved in regulating Yap activity *in vivo* during regeneration, we performed intraperitoneal injections of Jasplakinolide (Jasp), an inducer of F-actin polymerization and stabilization (Bubb et al., 1994; Reddy et al., 2013), in 72hpa Alpha-Catenin transgenics. To confirm that Jasp injection was leading to F-actin interference, we performed immunostainings against phosphorylated Ezrin/Radixin/Moesin. This antibody was used since it detects F-actin similarly to phalloidin, with the benefit of not occupying the same binding site of Jasp (Bubb et al., 1994). In contrast to DMSO controls, Jasp injected fins had lost the characteristic cortical F-actin localization in blastema distal tips, indicating that Jasp effectively acts on F-actin (Fig. S7G-J). Next we accessed Yap intracellular localization through immunostainings and observed that it was affected as early as 30 minutes after Jasp injection. Nuclear translocation of Yap was induced throughout the blastema in contrast to DMSO controls (Fig. 7A-B), which was particularly evident in distal regions of Jasp treated animals (Fig. 7C-E, compare DMSO XZ Distal with JASP XZ Distal). To confirm that this Yap nuclear translocation had an impact in its activation state, we performed qPCR for its target gene *ctgfa*,

in Jasp versus DMSO injected animals. This analysis showed that at 30 minutes of Jasp injection, *ctgfa* transcription levels were not readily affected in the blastema; however, by 2 hours post Jasp injection *ctgfa* was significantly upregulated when compared to DMSO animals (Fig. 7F). This suggests that disrupting F-actin dynamics overrides the mechanical cues provided by high cell density in the blastema distal tip, exerting influence on Yap activation. We also found that Alpha-Catenin distal accumulation is not altered upon Jasp treatment (Fig. 7G-J), indicating that Alpha-Catenin is not directly affected upon F-actin manipulation in the blastema. Altogether, these observations show that F-actin is an upstream regulator of Yap *in vivo*, controlling its activation during regeneration.

Discussion

Our study identifies an *in vivo* mechanism that regulates Yap activity within the zebrafish caudal fin blastema based on cell density differences along the regenerating tissue. The mesenchymal cells seem to respond to a mechanotransduction process that involves changes in cell morphology, junction assembly and cytoskeleton remodeling, which together lead to a graded control of tissue growth via Yap, the Hippo pathway effector.

Once formed, the blastema exhibits spatial compartmentalization (Nechiporuk and Keating, 2002). We show that Yap intracellular localization associates with these areas and could account for the different levels of proliferation described. Remarkably, the same Yap dynamics also correlates with the degree of cell density along the blastema PD axis. In distal high cell density domains, Yap is mainly cytoplasmic (inactive), while in proximal lower cell density domains, Yap is largely nuclear (active). The functional relevance of Yap intracellular localization was confirmed by genetic manipulation: expression of a constitutively active form of Yap leads to more proliferation, while expression of a Yap dominant negative construct results in the opposing phenotype. The effects of Yap manipulation are not only restricted to proliferation, but also influence the expression of several signaling factors. Importantly, the size

of the blastema is reduced in both cases, indicating that Yap is on top of a complex network of tissue growth regulation during regeneration, not limited to proliferation control.

Our observations of different levels of cell density (i.e. confluence) in the blastema suggest a mechanism of contact inhibition of proliferation, which to our knowledge has not been described before in regeneration or other *in vivo* tissue repair contexts. Recently, *in vitro* studies have proposed that Yap activation is hierarchically controlled by different upstream cues depending on culture confluence (Aragona et al., 2013). Interestingly in our *in vivo* system, the distal mesenchymal cells that exhibit high density and cytoplasmic Yap show multiple features that might contribute to Yap inactivation. These cells present rounder cell morphology, show Alpha-Catenin buildup, have increased activated Mst1/2 and Lats1/2 and display changes in F-actin localization. This suggests that a combination of several mechanical and signaling mechanisms exist to robustly inactivate Yap in the distal blastema. The initial step in the cascade of events leading to Yap inactivation in the distal tip needs further investigation, but it is conceivable that it depends primarily on the increase of density and cell contacts. The cause for cells accumulating distally is yet unclear, possibly being a structural consequence of the surrounding epithelial layers that impose physical constraints to the mesenchyme.

The membrane recruitment of Alpha-Catenin as a consequence of high cell density, resembles the process described in the mouse epidermis (Schlegelmilch et al., 2011); importantly, it may lead to the cortical repositioning of F-actin that in turn drives Yap inactivation. Interestingly, if we consider that less substrate contacts with the ECM are a consequence of high cell density, in which blastema cells become rounder, this should also cause F-actin relocation to the cell cortex and exclusion of Yap from the nucleus. We can only speculate about the possible mechanical contribution of ECM stiffness towards Yap inactivation, but it is tempting to associate blastema high cell density zones with possible soft substrates in which there is low mechanical tension conferred by the ECM. This would enable the system to have multiple ways of directing F-actin to the cell cortex and consequently inactivating Yap distally (Gumbiner and Kim, 2014).

Importantly, we show for the first time that F-actin plays a major role in mediating the influence of the blastema environment on Yap subcellular distribution *in vivo*.

F-actin has been shown to act as a mechanotransducer in other systems (Romet-Lemonne and Jégou, 2013; Heisenberg and Bellaïche, 2013), therefore it may be directly involved in sensing the mesenchymal cell density state and translate that into Yap activation. Additionally, Alpha-Catenin may act upstream of F-actin, possibly being a primary mechanosensor in response to density changes, as its recruitment in distal blastemas is unaffected upon F-actin manipulation; nevertheless further studies are necessary to understand this mechanism.

High cell density in the blastema appears to play an instructive role in the distal inactivation of Yap; however, it is unlikely that low cell density is the initial Yap activation trigger, rather being a required permissive step. The first signs of Yap activation were observed at 6hpa when cell migration towards the stump had not started; hence blastema density is unlikely to be considerably lower than the uncut mesenchymal tissue where Yap is inactive (Fig. 1A-C). Yap activation could be linked to the presence of F-actin in the mesenchyme or with secreted growth factors, such as WNT, which is early activated upon amputation and known for interplay with the Hippo pathway (Imajo et al., 2012; Rosenbluh et al., 2012; Stoick-Cooper et al., 2007).

Our finding that Yap signaling appears to be inhibited in uninjured, fully differentiated caudal fins supports the idea that Yap has a specific function during regeneration, when there is a need for precise control of tissue growth. This apparent prerequisite of a less differentiated environment is consistent with observations in other systems, in which Yap experimental manipulation leads to phenotypes in tissues that are not fully differentiated. This is the case during embryonic development, adult contexts involving stem cell niches and in cancer models, all situations where cell plasticity is enhanced (Hiemer and Varelas, 2013). This is suggestive of multiple levels of Yap regulation in differentiated tissues.

The coordination between a number of signaling pathways and morphogens during fin regeneration is essential to guarantee robustness in restoring correct final size. Importantly, our work proposes that mechanical forces, conferred by heterogeneous cell densities within the blastema, are also crucial for regeneration. By a process of mechanotransduction, mediated via Alpha-Catenin and F-actin, Yap regulation and therefore blastema growth are tightly balanced. This work thus reinforces a central physiological role for this Hippo pathway member *in vivo*.

Materials and Methods

Ethics Statement

All experiments were approved by the Animal User and Ethical Committees at Instituto Medicina Molecular and Instituto Gulbenkian Ciência, according to European Union directives and Portuguese law (Directive 2010/63/EU, Decreto-Lei 113/2013).

Zebrafish lines and fin amputation

All zebrafish (*Danio rerio*) lines used were maintained in a re-circulating system with a 14h/day, 10h/night cycle at 28°C. Experiments were performed in 3-9 months old wild type AB strain adults. All fin amputations were performed in fish anaesthetized in 160mg/mL MS-222 (Sigma) using a scalpel as described (Poss et al., 2000). Regeneration proceeded until defined time points at 33°C, except for heat-shock experiments. For those, transgenics and siblings were maintained at 28°C and heat-shocked once daily at 38°C for 1h, by water bath incubation. Subsequently fish were transferred to 28°C until desired time points. All live imaging was done in anaesthetized fish, with images acquired using a Zeiss V12-Lumar with a Zeiss digital camera. For transgenic generation, see Supplementary Materials and Methods.

Chemical treatments

For Jasplakinolide (Jasp)(Sta Cruz Biotechnology) treatments, 72hpa ctnna-Citrine fish were injected intraperitoneally with 10µL/g-fish of 1mM Jasp working solution (final concentration of 7,1µg Jasp/g-fish) in dimethyl sulfoxide (DMSO, Sigma). Fish were injected 30min or 2h prior to fixation with 30G U-100 insulin syringes (BD Micro-Fine). Control fish were injected in parallel with an equivalent volume of DMSO. EdU (5-ethynyl-2'-deoxyuridine) injections were performed as described (Blum and Begemann, 2011), in 72hpa CA-yap transgenics and siblings. Fish were injected 1h prior to fixation as above. Fins were fixed in 4% paraformaldehyde (Sigma) in PBS o/n and processed for cryosections or were pooled for RNA extraction directly in Trizol reagent (see Supplementary Materials and Methods).

Image analysis

For all image analysis, maximum intensity z-stack projections were made using ImageJ software, except when noted. For concatenation of images along the PD axis of the same longitudinal section, the ImageJ plugin 3D Stitching was used. XZ projections were performed with Dynamic Reslice in ImageJ, using synchronized channels. All error bars in graphs correspond to the standard deviation of the mean. For proliferation, Yap intracellular localization quantifications, cell density, cell morphology and intercellular mesenchymal space measurements see Supplementary Materials and Methods.

In situ hybridization

Whole-mount *in situ* hybridizations in caudal fins and embryos were performed as described (Sousa et al., 2011; Thisse and Thisse, 2008). Genes were PCR-cloned by TA overhangs in PGEM-T-easy (Promega) by using primers (Table S2) and 5dpf zebrafish total cDNA. *cmlc2* probe was a gift (Yelon et al., 1999). DIG-labeled antisense RNA probes for all studied genes were synthesized as described (Henrique et al., 1995)(Table S3). Images of *in situ* hybridizations were obtained with a Leica Z6APO stereomicroscope, with a Leica DFC490 digital camera or a Zeiss V12-Lumar with a Zeiss digital camera.

Immunofluorescence

This protocol was adapted from (Mateus et al., 2012) with the following modifications: after o/n fixation with 4% paraformaldehyde, fins were saturated in 30% sucrose (Sigma) in PBS o/n, then embedded in 7,5% gelatin (Sigma)/ 15% sucrose in PBS and subsequently frozen in liquid nitrogen. Longitudinal sections were cut at 12µm using a Microm cryostat and maintained at -20°C afterwards. Sections in slides were thawed 15min at room temperature, washed twice in PBS at 37°C for 10min, washed once in 0.1M glycine (Sigma) in PBS for 10min, followed by

acetone permeabilization and onwards as described. For EdU detection, directions from the kit Click-iT (C10637, Invitrogen) were followed. For Tunel detection, directions from In situ Cell Death Detection Kit, Fluorescein (Roche) were followed. Cryosections were counterstained with DAPI (0.001mg/mL in PBS, Sigma). In stainings with phalloidin (1:200, conjugated with Alexa Fluor 568, Invitrogen), upon fixation there was no methanol transfer and fins proceeded directly to PBS-30% sucrose. Sections were mounted with DAKO Fluorescent Mounting Media and imaged using a Zeiss LSM710 confocal microscope with a C-Apochromat 40x water objective. The antibodies used are listed in Table S4.

Author Contributions

RM performed all experiments with help of RL, GB, FV, AF. RM, RL, GB, AJ conceived and designed experiments, performed data analysis. RM, GB established the *ctgfa*:eGFP line and YF the hsp70:RFP-CAYap and hsp70:DNyap lines. RM, AJ prepared the manuscript.

Acknowledgements

We are grateful to Kenneth Poss for support and sharing Yap transgenics. The authors thank Lara M.Carvalho and Aida Barros for fish care. We thank Lara C.Carvalho, Sara Sousa, Maria Gagliardi for reading the manuscript and Telmo Pereira for data analysis. This work was supported by funding from Fundação para a Ciência e Tecnologia (SFRH/BD/62126/2009,PTDC/BEX-BID/1176/2012) and Agence Nationale de la Recherche (ANR-11-BSV5-0021).

References

- Aragona, M., Panciera, T., Manfrin, A., Giullitti, S., Michielin, F., Elvassore, N., Dupont, S. and Piccolo, S.** (2013). A Mechanical Checkpoint Controls Multicellular Growth through YAP/TAZ Regulation by Actin-Processing Factors. *Cell* 1–13.
- Azevedo, A. S., Grotek, B., Jacinto, A., Weidinger, G. and Saúde, L.** (2011). The Regenerative Capacity of the Zebrafish Caudal Fin Is Not Affected by Repeated Amputations. *PLoS One* 6, e22820.
- Blum, N. and Begemann, G.** (2011). Retinoic acid signaling controls the formation, proliferation and survival of the blastema during adult zebrafish fin regeneration. *Development* 116, 107–116.
- Bubb, M. R., Senderowicz, A. M., Sausville, E. A., Duncan, K. L. and Korn, E. D.** (1994). Jasplakinolide, a cytotoxic natural product, induces actin polymerization and competitively inhibits the binding of phalloidin to F-actin. *J. Biol. Chem.* 269, 14869–71.
- Cai, J., Zhang, N., Zheng, Y., de Wilde, R. F., Maitra, A. and Pan, D.** (2010). The Hippo signaling pathway restricts the oncogenic potential of an intestinal regeneration program. *Genes Dev.* 24, 2383–8.
- Choi, W.-Y., Gemberling, M., Wang, J., Holdway, J. E., Shen, M.-C., Karlstrom, R. O. and Poss, K. D.** (2013). In vivo monitoring of cardiomyocyte proliferation to identify chemical modifiers of heart regeneration. *Development* 140, 660–6.
- Cole, L. K. and Ross, L. S.** (2001). Apoptosis in the developing zebrafish embryo. *Dev Biol.* 240(1), 123–42.

- Dickmeis, T., Plessy, C., Rastegar, S., Aanstad, P., Herwig, R., Chalmel, F., Fischer, N. and Strähle, U.** (2004). Expression profiling and comparative genomics identify a conserved regulatory region controlling midline expression in the zebrafish embryo. *Genome Res.* **14**, 228–38.
- Dong, J., Feldmann, G., Huang, J., Wu, S., Zhang, N., Comerford, S. A., Gayyed, M. F., Anders, R. A., Maitra, A. and Pan, D.** (2007). Elucidation of a universal size-control mechanism in *Drosophila* and mammals. *Cell* **130**, 1120–33.
- Dupont, S., Morsut, L., Aragona, M., Enzo, E., Giulitti, S., Cordenonsi, M., Zanconato, F., Le Digabel, J., Forcato, M., Bicciato, S., et al.** (2011). Role of YAP/TAZ in mechanotransduction. *Nature* **474**, 179–183.
- Fernández, B. G., Gaspar, P., Brás-pereira, C., Jezowska, B., Rebelo, S. R. and Janody, F.** (2011). Actin-Capping Protein and the Hippo pathway regulate F-actin and tissue growth in *Drosophila*. *Development* **138**, 2337–46.
- Fernando, C. A., Conrad, P. A., Bartels, C. F., Marques, T., To, M., Balow, S. A., Nakamura, Y. and Warman, M. L.** (2010). Temporal and spatial expression of CCN genes in zebrafish. *Dev. Dyn.* **239**, 1755–67.
- Fukui, H., Terai, K., Nakajima, H., Chiba, A., Fukuhara, S. and Mochizuki, N.** (2014). S1P-Yap1 signaling regulates endoderm formation required for cardiac precursor cell migration in zebrafish. *Dev Cell.* **31(1)**, 128–36.
- Gumbiner, B. M. and Kim, N.-G.** (2014). The Hippo-YAP signaling pathway and contact inhibition of growth. *J. Cell Sci.* **127**, 709–717.
- Hayashi, S., Tamura, K. and Yokoyama, H.** (2014). Yap1, transcription regulator in the Hippo signaling pathway, is required for *Xenopus* limb bud regeneration. *Dev. Biol.* **388**, 57–67.

- Heisenberg, C. and Bellaïche, Y.** (2013). Forces in tissue morphogenesis and patterning. *Cell* **153**, 948–62.
- Henrique, D., Adam, J., Myat, A., Chitnis, A., Lewis, J. and Ish-Horowicz, D.** (1995). Expression of a Delta homologue in prospective neurons in the chick. *Nature* **375**, 787–790.
- Hiemer, S. E. and Varelas, X.** (2013). Stem cell regulation by the Hippo pathway. *Biochim. Biophys. Acta* **1830**, 2323–34.
- Hu, J., Sun, S., Jiang, Q., Sun, S., Wang, W., Gui, Y. and Song H.** (2013). Yes-Associated Protein (Yap) is required for early embryonic development in zebrafish (*Danio rerio*). *International Journal of Biological Sciences* **9(3)**:267-278.
- Huang, J., Wu, S., Barrera, J., Matthews, K. and Pan, D.** (2005). The Hippo signaling pathway coordinately regulates cell proliferation and apoptosis by inactivating Yorkie, the *Drosophila* Homolog of YAP. *Cell* **122**, 421–34.
- Imajo, M., Miyatake, K., Iimura, A., Miyamoto, A. and Nishida, E.** (2012). A molecular mechanism that links Hippo signalling to the inhibition of Wnt/ β -catenin signalling. *EMBO J.* **31**, 1–14.
- Jażwińska, A., Badakov, R. and Keating, M. T.** (2007). Activin-betaA signaling is required for zebrafish fin regeneration. *Curr. Biol.* **17**, 1390–5.
- Knopf, F., Hammond, C., Chekuru, A., Kurth, T., Hans, S., Weber, C. W., Mahatma, G., Fisher, S., Brand, M., Schulte-Merker, S., et al.** (2011). Bone Regenerates via Dedifferentiation of Osteoblasts in the Zebrafish Fin. *Dev. Cell* **20**, 713–24.

- Kujawski, S., Lin, W., Kitte, F., Börmel, M., Fuchs, S., Arulmozhivarman, G., Vogt, S., Theil, D., Zhang, Y. and Antos, C. L.** (2014). Calcineurin regulates coordinated outgrowth of zebrafish regenerating fins. *Dev. Cell* **28**, 573–87.
- Lee, Y., Grill, S., Sanchez, A., Murphy-Ryan, M. and Poss, K. D.** (2005). Fgf signaling instructs position-dependent growth rate during zebrafish fin regeneration. *Development* **132**, 5173–83.
- Lee, Y., Hami, D., De Val, S., Kagermeier-Schenk, B., Wills, A. A., Black, B. L., Weidinger, G. and Poss, K. D.** (2009). Maintenance of blastemal proliferation by functionally diverse epidermis in regenerating zebrafish fins. *Dev. Biol.* **331**, 270–80.
- Mahoney, W. M., Hong, J., Yaffe, M. B. and Farrance, I. K. G.** (2005). The transcriptional co-activator TAZ interacts differentially with transcriptional enhancer factor-1 (TEF-1) family members. *Biochem. J.* **388**, 217–25.
- Mateus, R., Pereira, T., Sousa, S., de Lima, J. E., Pascoal, S., Saúde, L. and Jacinto, A.** (2012). In vivo cell and tissue dynamics underlying zebrafish fin fold regeneration. *PLoS One* **7**, e51766.
- Miesfeld, J. B. and Link, B. A.** (2014). Establishment of transgenic lines to monitor and manipulate Yap/Taz-Tead activity in zebrafish reveals both evolutionarily conserved and divergent functions of the Hippo pathway. *Mech Dev.* **133**, 177–88.
- Morgan, T. H.** (1901). Regeneration. *New York, Macmillan Company; London, Macmillan Co., Ltd.*
- Nechiporuk, A. and Keating, M. T.** (2002). A proliferation gradient between proximal and msxb-expressing distal blastema directs zebrafish fin regeneration. *Development* **129**, 2607–17.

- Oh, H. and Irvine, K. D.** (2008). In vivo regulation of Yorkie phosphorylation and localization. *Development* **135**, 1081–8.
- Pan, D.** (2010). The hippo signaling pathway in development and cancer. *Dev. Cell* **19**, 491–505.
- Perathoner, S., Daane, J. M., Henrion, U., Seebohm, G., Higdon, C. W., Johnson, S. L., Nüsslein-Volhard, C. and Harris, M. P.** (2014). Bioelectric signaling regulates size in zebrafish fins. *PLoS Genet.* **10**, e1004080.
- Poleo, G., Brown, C. W., Laforest, L. and Akimenko, M. a** (2001). Cell proliferation and movement during early fin regeneration in zebrafish. *Dev. Dyn.* **221**, 380–90.
- Poss, K. D. D., Shen, J. and Keating, M. T. T.** (2000). Induction of *lef 1* during zebrafish fin regeneration. *Dev. Dyn.* **219**, 282–286.
- Reddy, P., Deguchi, M., Cheng, Y. and Hsueh, A. J. W.** (2013). Actin cytoskeleton regulates hippo signaling. *PLoS One* **8**, e73763.
- Romet-Lemonne, G. and Jégou, A.** (2013). Mechanotransduction down to individual actin filaments. *Eur. J. Cell Biol.* **92**, 333–8.
- Rosenbluh, J., Nijhawan, D., Cox, A. G. G., Li, X., Neal, J. T. T., Schafer, E. J. J., Zack, T. I. I., Wang, X., Tsherniak, A., Schinzel, A. C. C., et al.** (2012). β -Catenin-Driven Cancers Require a YAP1 Transcriptional Complex for Survival and Tumorigenesis. *Cell* **151**, 1457–1473.
- Santos-Ruiz, L., Santamaría, J. A. and Becerra, J.** (2005). Cytoskeletal dynamics of the teleostean fin ray during fin epimorphic regeneration. *Differentiation.* **73**, 175–87.

- Schlegelmilch, K., Mohseni, M., Kirak, O., Pruszk, J., Rodriguez, J. R., Zhou, D., Kreger, B. T., Vasioukhin, V., Avruch, J., Brummelkamp, T. R., et al. (2011). Yap1 Acts Downstream of a-Catenin to Control Epidermal Proliferation. *Cell* **144**, 782–795.
- Sousa, S., Afonso, N., Bensimon-Brito, A., Fonseca, M., Simões, M., Leon, J., Roehl, H., Cancela, M. L. and Jacinto, A. (2011). Differentiated skeletal cells contribute to blastema formation during zebrafish fin regeneration. *Development* **138**, 3897–905.
- Staley, B. K. and Irvine, K. D. (2010). Warts and yorkie mediate intestinal regeneration by influencing stem cell proliferation. *Curr. Biol.* **20**, 1580–7.
- Stewart, S., Gomez, A. W., Armstrong, B. E., Henner, A. and Stankunas, K. (2014). Sequential and Opposing Activities of Wnt and BMP Coordinate Zebrafish Bone Regeneration. *Cell Rep.* **7**, 1–17.
- Stewart, S. and Stankunas, K. (2012). Limited dedifferentiation provides replacement tissue during zebrafish fin regeneration. *Dev. Biol.* **365**, 339–49.
- Stoick-Cooper, C. L., Weidinger, G., Riehle, K. J., Hubbert, C., Major, M. B., Fausto, N. and Moon, R. T. (2007). Distinct Wnt signaling pathways have opposing roles in appendage regeneration. *Development* **134**, 479–89.
- Sugiyama, M., Sakaue-Sawano, A., Iimura, T., Fukami, K., Kitaguchi, T., Kawakami, K., Okamoto, H., Higashijima, S. and Miyawaki, A. (2009). Illuminating cell-cycle progression in the developing zebrafish embryo. *Proc. Natl. Acad. Sci. U. S. A.* **106**, 20812–7.
- Thisse, C. and Thisse, B. (2008). High-resolution in situ hybridization to whole-mount zebrafish embryos. *Nat. Protoc.* **3**, 59–69.

- Thummel, R., Burket, C. T. and Hyde, D. R.** (2006). Two different transgenes to study gene silencing and re-expression during zebrafish caudal fin and retinal regeneration. *ScientificWorldJournal*. **6 Suppl 1**, 65–81.
- Wada, K., Itoga, K., Okano, T., Yonemura, S. and Sasaki, H.** (2011). Hippo pathway regulation by cell morphology and stress fibers. *Development* **138**, 3907–14.
- Wehner, D., Cizelsky, W., Vasudevaro, M. D., Ozhan, G., Haase, C., Kagermeier-Schenk, B., Röder, A., Dorsky, R. I., Moro, E., Argenton, F., et al.** (2014). Wnt/ β -Catenin Signaling Defines Organizing Centers that Orchestrate Growth and Differentiation of the Regenerating Zebrafish Caudal Fin. *Cell Rep.* 1–15.
- Wills, A. A., Kidd, A. R., Lepilina, A. and Poss, K. D.** (2008). Fgfs control homeostatic regeneration in adult zebrafish fins. *Development* **135**, 3063–70.
- Xia, H., Qi, H., Li, Y., Pei, J., Barton, J., Blackstad, M., Xu, T. and Tao, W.** (2002). LATS1 tumor suppressor regulates G2/M transition and apoptosis. *Oncogene* **21**, 1233–41.
- Yagi, R., Chen, L. F., Shigesada, K., Murakami, Y. and Ito, Y.** (1999). A WW domain-containing yes-associated protein (YAP) is a novel transcriptional co-activator. *EMBO J.* **18**, 2551–62.
- Yelon, D., Horne, S. A. and Stainier, D. Y.** (1999). Restricted expression of cardiac myosin genes reveals regulated aspects of heart tube assembly in zebrafish. *Dev Biol.* **214(1)**, 23–37.
- Zhang, J., Ji, J.-Y., Yu, M., Overholtzer, M., Smolen, G. a, Wang, R., Brugge, J. S., Dyson, N. J. and Haber, D. a** (2009). YAP-dependent induction of amphiregulin identifies a non-cell-autonomous component of the Hippo pathway. *Nat. Cell Biol.* **11**, 1444–50.

Zhao, B., Wei, X., Li, W., Udan, R. S., Yang, Q., Kim, J., Xie, J., Ikenoue, T., Yu, J., Li, L., et al. (2007). Inactivation of YAP oncoprotein by the Hippo pathway is involved in cell contact inhibition and tissue growth control. *Genes Dev.* **21**, 2747–61.

Zhao, B., Ye, X., Yu, J. J., Li, L., Li, W., Li, S., Lin, J. D., Wang, C.-Y., Chinnaiyan, A. M., Lai, Z.-C., et al. (2008). TEAD mediates YAP-dependent gene induction and growth control. *Genes Dev.* **22**, 1962–71.

Žigman, M., Trinh, L. a, Fraser, S. E., Moens, C. B. and Zigman, M. (2010). Zebrafish neural tube morphogenesis requires Scribble-dependent oriented cell divisions. *Curr. Biol.* **21**, 79–86.

Figures

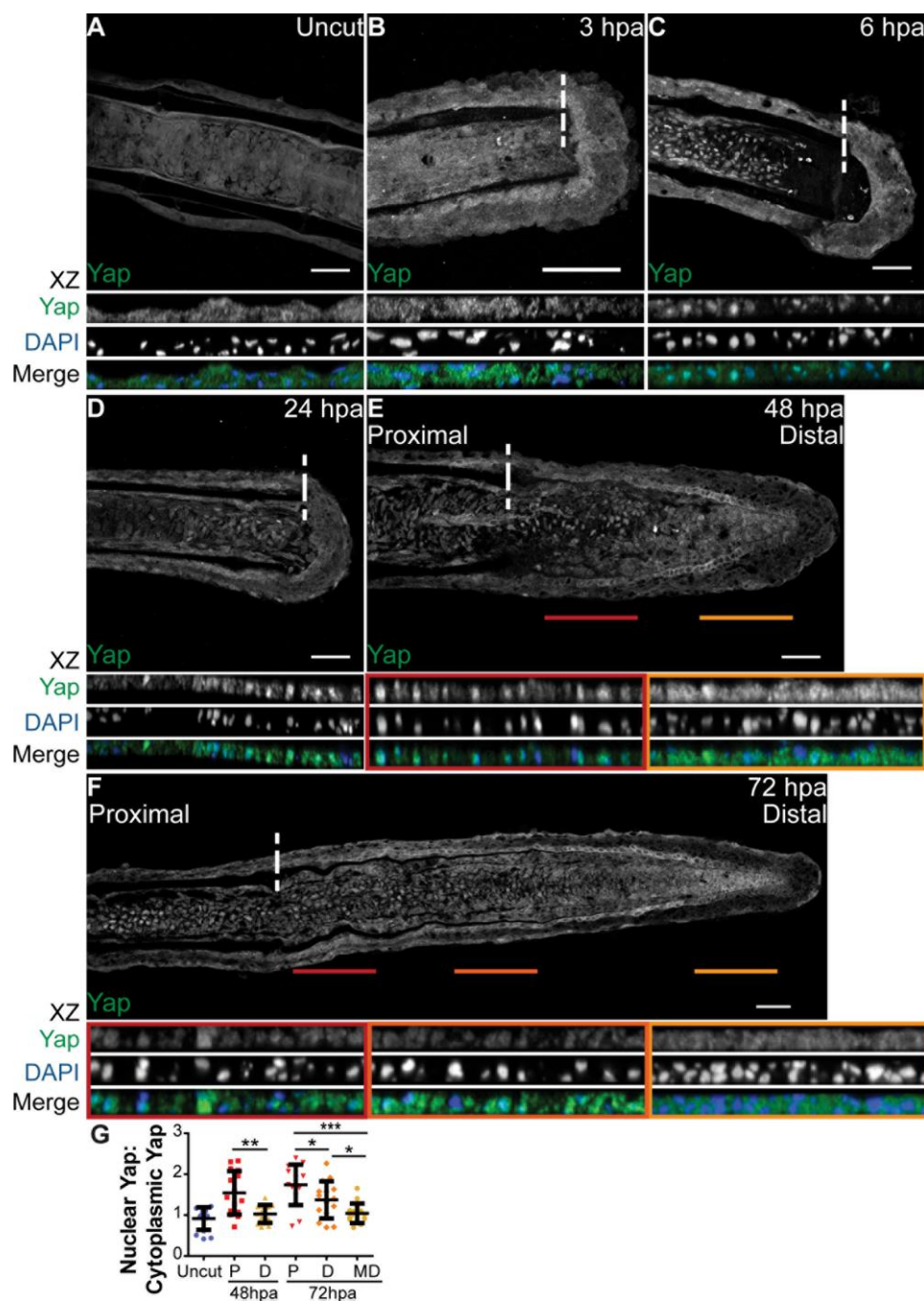


Fig. 1. Yap is present and highly dynamic during fin regeneration. A-F Representative immunostainings with anti-Yap in caudal fin longitudinal sections in several regenerative stages. A Uncut control; B 3hpa; C 6hpa; D 24hpa; E 48hpa; F 72hpa. XZ projections of mesenchymal regions highlight Yap intracellular localization. Distal (yellow) and proximal

(red) colored lines in 48hpa (E), and distal most (yellow), distal (orange) and proximal (red) colored lines in 72hpa (F), correspond to mesenchymal areas in the medial blastema where XZ projections were made in above sections. Dashed lines indicate amputation plane. n=10-15 sections; 5 fish/condition. Scale bars=50 μ m. **G** Quantification of Yap intracellular localization by expressing a ratio between average intensities of Nuclear Yap:Cytoplasmic Yap of XZ projections from blastemas at different time points. Higher ratios correspond to higher intensities of nuclear Yap. P corresponds to XZ of proximal (red); D to distal (orange); DM to distal most regions (yellow). *P value<0.05, **P value<0.01, ***P value<0.001; two tailed, non-parametric Mann-Whitney test. n=15 sections, 5 fish/condition.

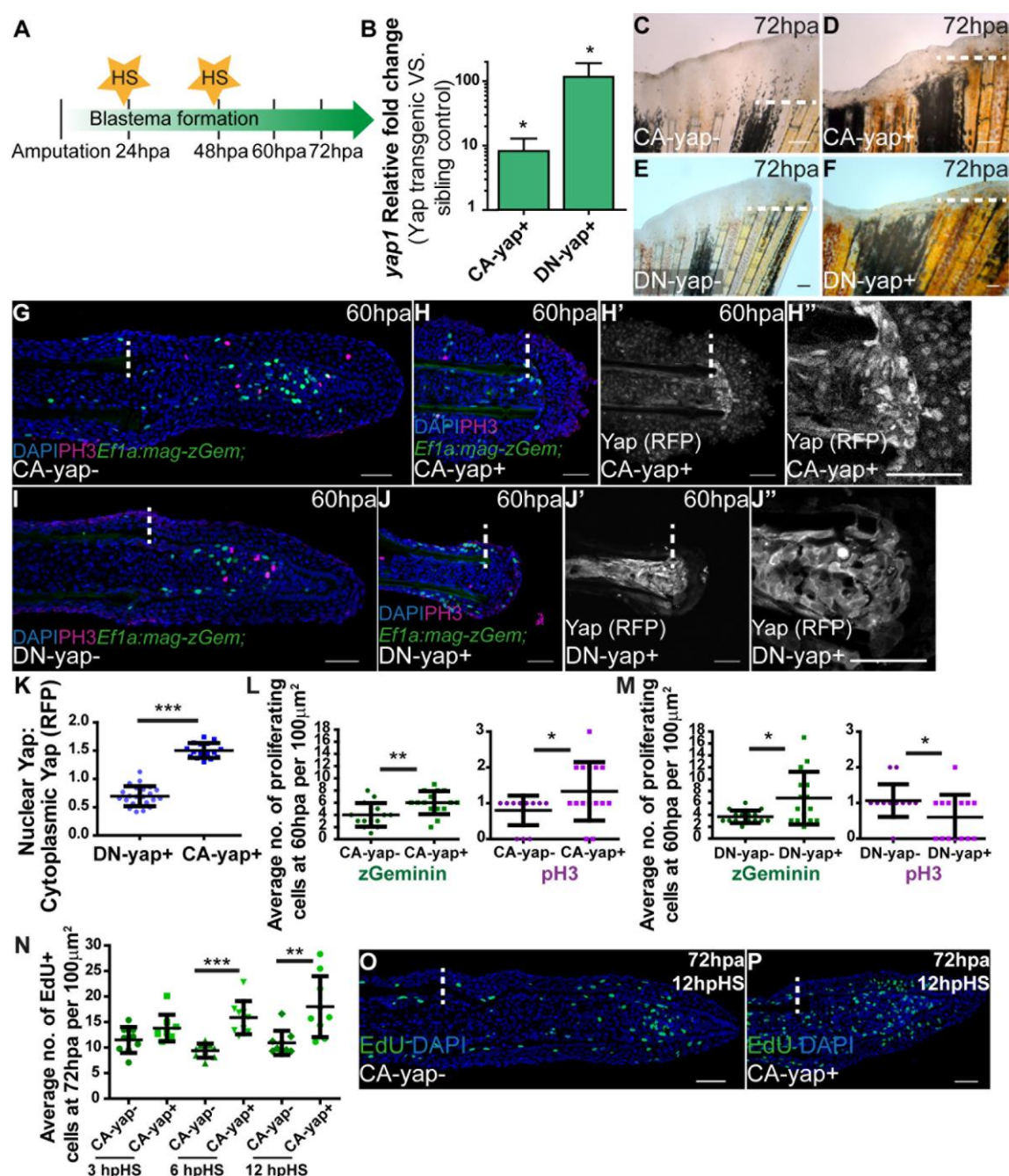


Fig. 2. Yap influences the proliferation in the blastema. **A** Experimental outline of heat-shock protocol used to access Yap functionality during regeneration. After amputations fish were allowed to regenerate 24h, time when the first heat-shock was performed. A second heat-shock at 48hpa was applied and phenotypes were accessed at 60hpa or 72hpa. The same protocol was applied to sibling controls. **B-C** qPCR determination of *yap1* expression levels in blastemas of Yap transgenics versus respective siblings upon single heat-shock at 72hpa.

Relative expression in **B** CA-yap positive, **C** DN-yap positive transgenics. RNA extraction was performed at 2hpHS. *P value<0.01; two tailed, non-parametric paired Wilcoxon test, logarithmic scale, base 10. **C-F** Representative brightfield images of Yap transgenics and siblings at 72hpa after protocol applied in A. **C** CA-yap control; **D** CA-yap positive; **E** DN-yap control; **F** DN-yap positive. n=5 fish/condition. Scale bars=200µm. **G-J** Representative immunofluorescence with anti-pH3 in 60hpa longitudinal sections of double transgenics Eflα:mag-zGeminin; CA-yap/DN-yap and siblings after protocol defined in A. **G** CA-yap control; **H** CA-yap positive; **I** DN-yap control; **J** DN-yap positive. **H'-H'', J'-J''** Corresponding transgenic CA-Yap/DN-Yap RFP expression with zoomed images after protocol in A, at 60hpa. Siblings do not show RFP expression. Scale bars=50µm. **K** Quantification of Yap-RFP intracellular localization in CA-yap/DN-yap transgenics by expressing a ratio between average intensities of Nuclear Yap: Cytoplasmic Yap of XZ projections of respective mesenchymal cells. ***P value<0.001; two tailed, non-parametric Mann-Whitney test. n=16-23 sections, 3 fish/condition. **L, M** Quantification of average proliferation labeled with Geminin and pH3 occurring per 100µm² in Eflα:mag-zGeminin; CA-yap/DN-yap and siblings, at 60hpa. *P value<0.05, **P value<0.01; two tailed, non-parametric Mann-Whitney test. n=15 sections, 3 fish/condition. **N** Quantification of average EdU positive cells occurring per 100µm² in CA-yap and siblings, at 72hpa in different times post heat-shock. **P value<0.01, ***P value<0.001; two tailed, non-parametric Mann-Whitney test. n=9 sections, 3 fish/condition. **O-P** Representative immunofluorescence with EdU in 72hpa longitudinal sections of CA-yap and siblings after 12hpHS. **O** CA-yap control; **P** CA-yap positive. Scale bars=50µm. Dashed lines indicate amputation plane.

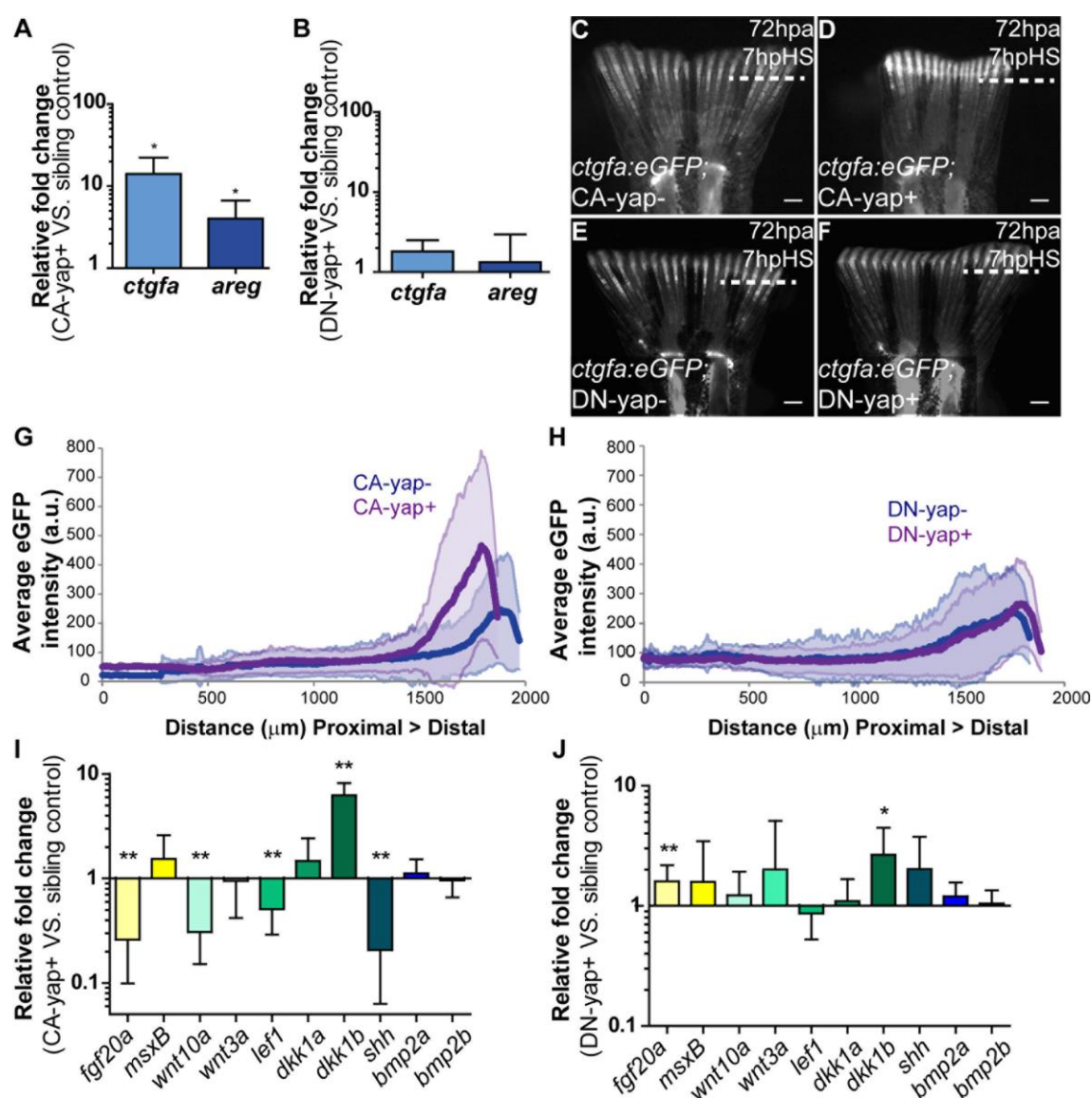


Fig. 3. Transcriptional gene regulation induced by Yap. A-B qPCR determination of *ctgfa* and *areg* expression levels in blastemas of Yap transgenics versus siblings upon single heat-shock at 72hpa. Relative expression in **A** CA-yap positive, **B** DN-yap positive transgenics. *P value<0.01; two tailed, non-parametric paired Wilcoxon test, logarithmic scale, base 10. **C-F** Representative *ctgfa* expression in double transgenics *ctgfa*:eGFP; CA-yap/DN-yap and siblings upon heat-shock at 72hpa, at 7hpHS. **C** CA-yap control; **D** CA-yap positive; **E** DN-yap control; **F** DN-yap positive. n=5 fish/condition. Scale bars=500μm. Dashed lines indicate amputation plane. **G-H** Quantification of average eGFP intensity (in arbitrary units, a.u.) of individual rays

including blastemas along the PD axis (μm) of double transgenics *ctgfa:eGFP*; CA-yap/DN-yap and siblings. **G** CA-yap positive and siblings; **H** DN-yap and siblings. n=80-90 rays, 5 fish/condition; shadows indicate the s.e.m for each curve. **I-J** qPCR determination of *fgf20a*, *msxB*, *wnt10a*, *wnt3a*, *lef1*, *dkk1a*, *dkk1b*, *shh*, *bmp2a*, *bmp2b* expression levels in Yap transgenics versus siblings upon single heat-shock at 72hpa. Relative expression in **I** CA-yap positive, **J** DN-yap positive transgenics. *P value<0.05, **P value<0.01; two tailed, non-parametric paired Wilcoxon test, logarithmic scale, base 10. All RNA extractions were performed at 2hpHS.

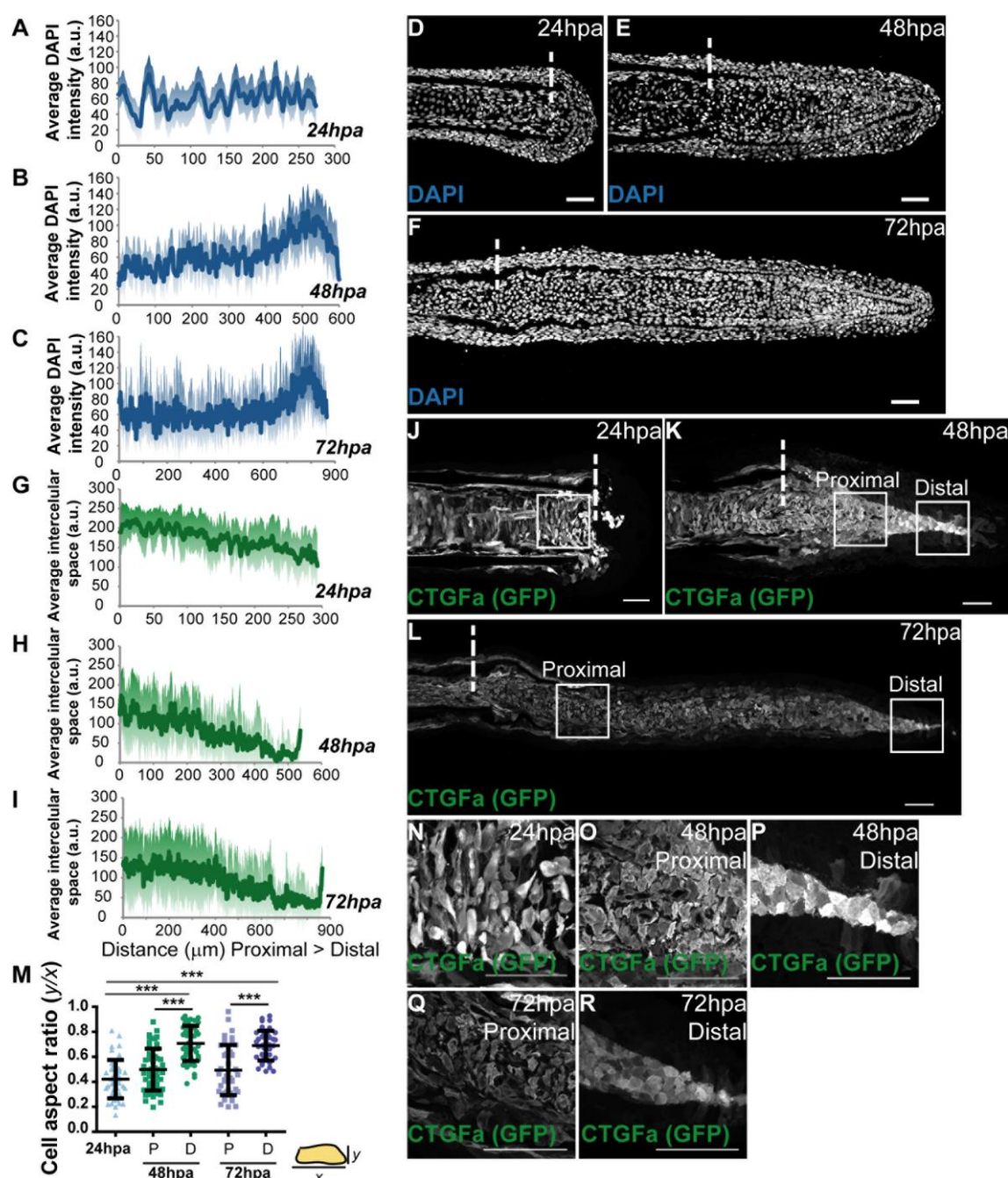


Fig. 4. Mesenchymal cell density and morphology are altered according to the regenerative stage. **A, B, C** Quantification of average DAPI intensity (in arbitrary units, a.u.) in mesenchymal cells along the PD axis (μm) of blastemas at 24hpa (**A**), 48hpa (**B**), 72hpa (**C**). n=7 sections, 3 fish/condition. **D, E, F** Representative DAPI stained longitudinal sections. **D** 24hpa; **E** 48hpa; **F** 72hpa. **G, H, I** Quantification of average space (a.u.) between mesenchymal

cells along the PD axis (μm) at 24hpa (**G**), 48hpa (**H**), 72hpa (**I**). n=9 sections; 3 fish/condition; **J, K, L** Representative anti-GFP stained longitudinal sections of *ctgfa:eGFP* transgenics. **J** 24hpa; **K** 48hpa; **L** 72hpa. **M** Quantification of average cell aspect ratio of mesenchymal cells at 24, 48 and 72hpa, in which y is the minor axis of the cell and x the major cell axis. A perfect circular shape corresponds to a ratio between y and x of 1. P corresponds to proximal; D to distal regions. ***P value<0.0001; two tailed, non-parametric Mann-Whitney test. n=45 cells/condition; 5 cells randomly selected/image; 9 sections; 3 fish/condition. **N-R** Corresponding zooms of J, K, L highlight cell morphology of blastema cells at 24hpa (**N**), 48hpa proximally (**O**), distally (**P**), 72hpa proximally (**Q**) distally (**R**). Dashed lines indicate amputation plane. Scale bars=50 μm . Medial blastema areas were considered for all measurements: shadows indicate the s.e.m for each curve.

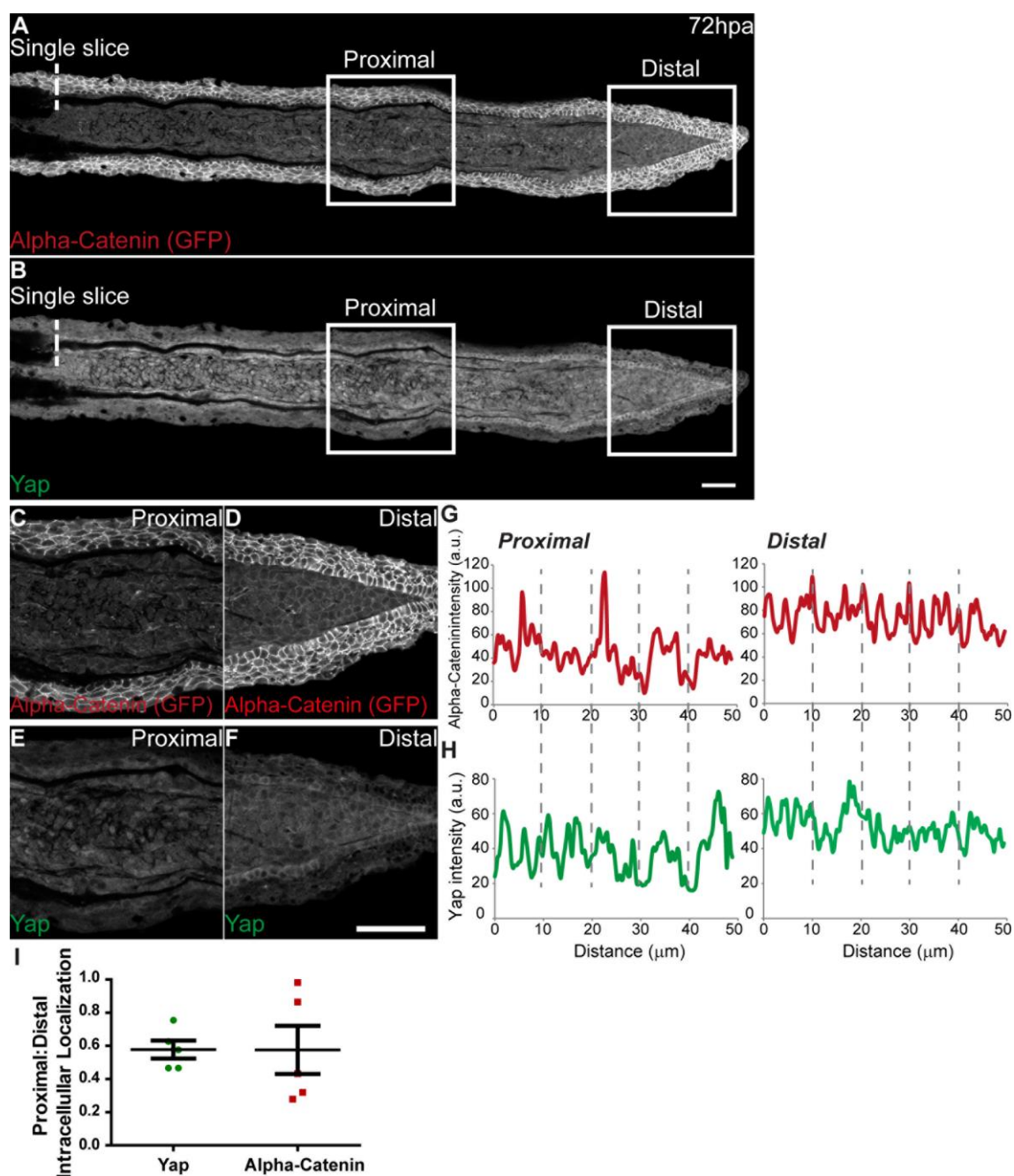


Fig. 5. Alpha-Catenin accumulates in distal blastema regions where Yap is mainly cytoplasmic. Representative immunofluorescence with anti-Yap and anti-GFP in 72hpa longitudinal sections of Alpha-Catenin transgenics. Owing to stronger expression intensity, transgenics were used instead of the Alpha-Catenin antibody. **A** Alpha-Catenin; **B** Corresponding Yap expression. **C-F** Zoomed areas represented by squares in A-B. Proximal (**C**)

and distal (**D**) images from A showing Alpha-Catenin. Corresponding proximal (**E**) and distal (**F**) images from B showing Yap. **G-H** Corresponding proximal and distal intensity profiles (in arbitrary units, a.u.) of medial mesenchymal cells shown in C-F. **G** Average intensity of Alpha-Catenin; **H** Average intensity of Yap. **I** Quantification of Yap and Alpha-Catenin changes in intracellular localization in PD regions by expressing a ratio between average intensities of Proximal:Distal Yap or Alpha-Catenin of XZ projections of respective mesenchymal cells. Dashed lines indicate amputation plane. n=5 sections, 3 fish. Scale bars=50 μ m.

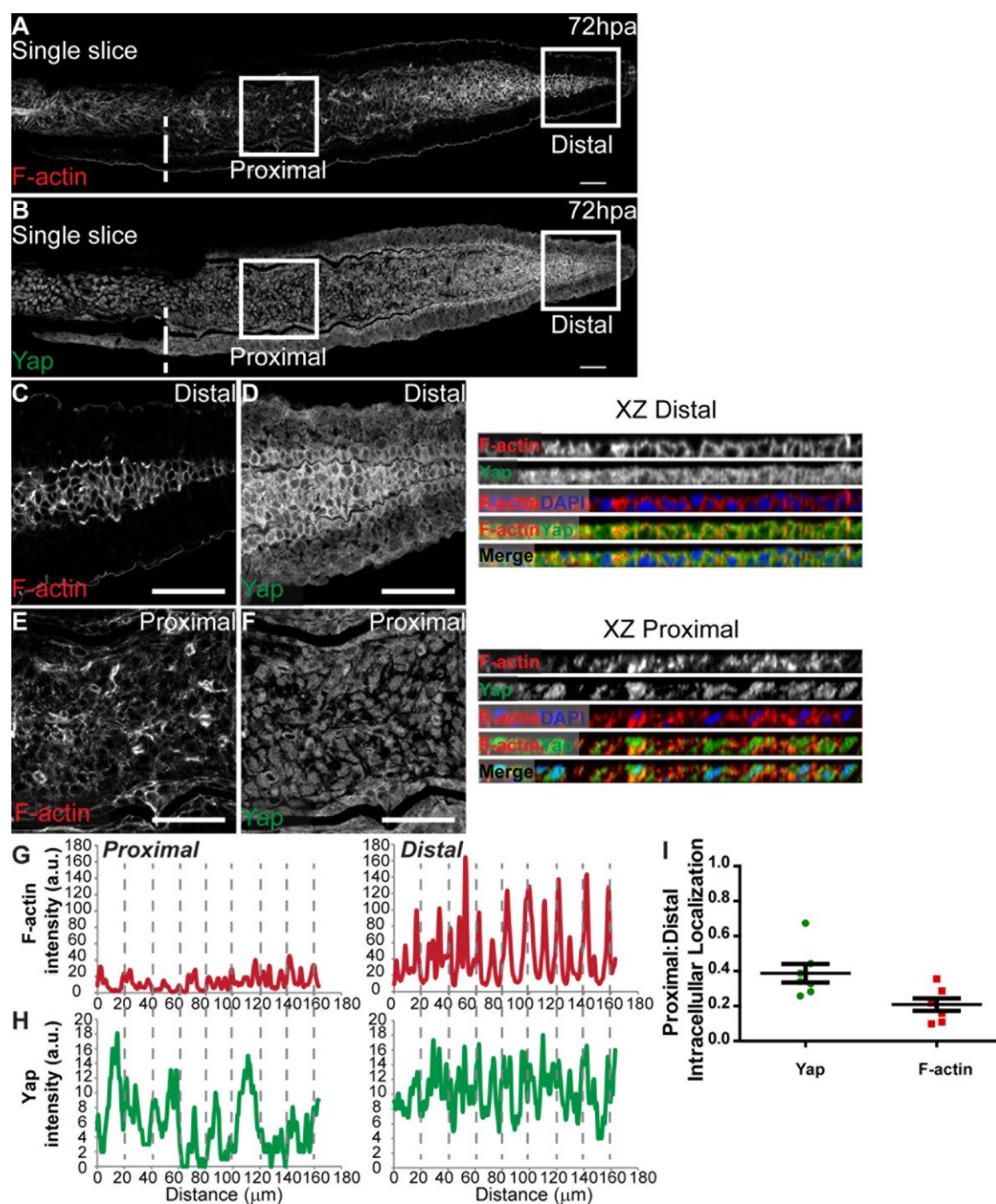


Fig. 6. Differential proximo-distal expression of F-actin associates with Yap intracellular location. Representative immunofluorescence with anti-Yap and phalloidin (F-actin) in 72hpa longitudinal sections. **A** F-actin; **B** Corresponding Yap expression. **C-F** Zoomed areas represented by squares in A-B. Proximal (**E**) and distal (**C**) images from A showing F-actin.

Corresponding proximal (**F**) and distal (**D**) images from B showing Yap. Single color and merged XZ projections of distal C-D and proximal E-F blastemas highlight intracellular localization. **G-H** Corresponding proximal and distal intensity profiles (in arbitrary units, a.u.) of XZ projections represented. **G** Average intensity of F-actin; **H** Average intensity of Yap. **I** Quantification of Yap and F-actin changes in intracellular localization in PD regions by expressing a ratio between average intensities of Proximal:Distal Yap or F-actin of XZ projections of respective mesenchymal cells. Dashed lines indicate amputation plane. n=7 sections, 5 fish. Scale bars=50 μ m.

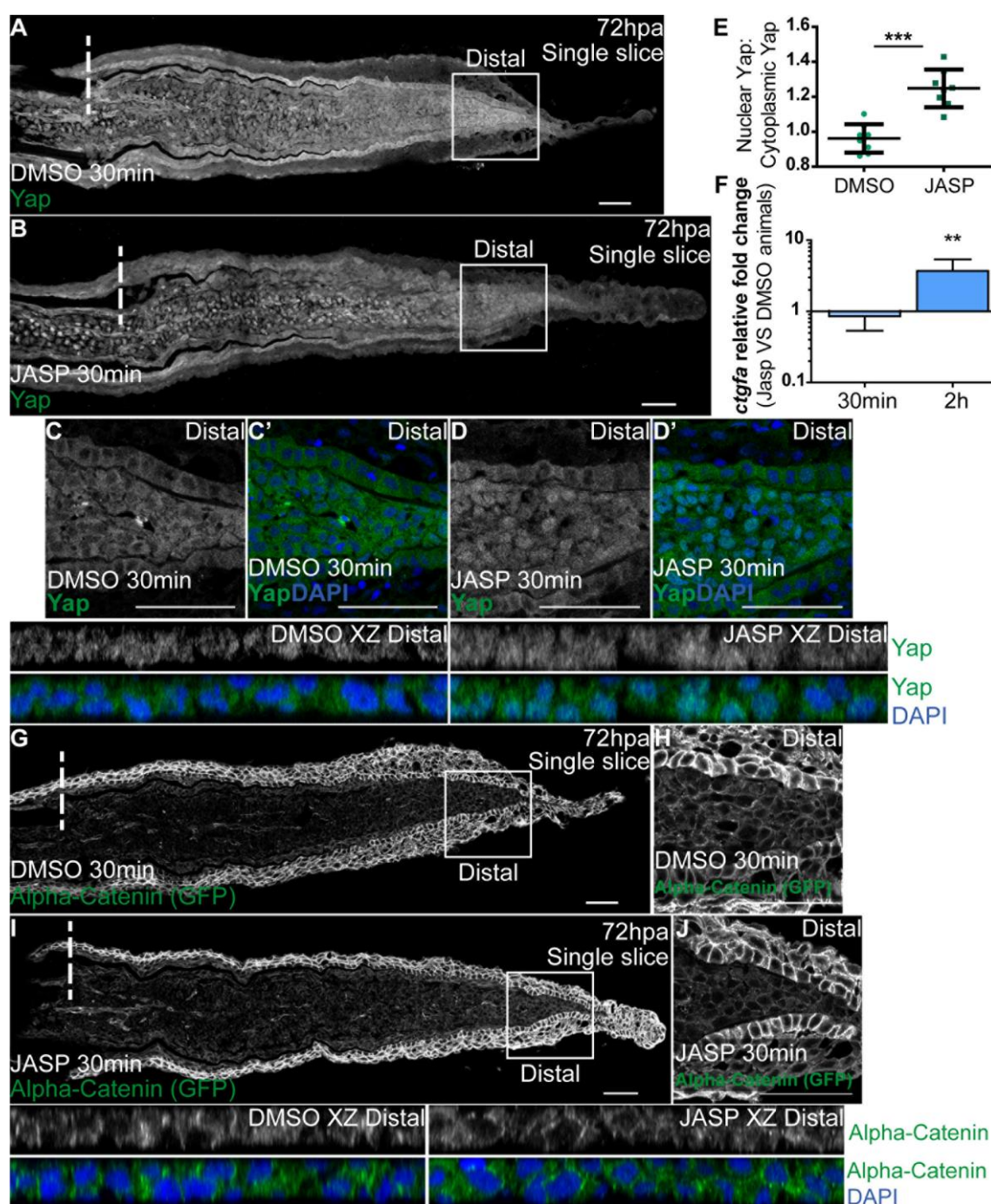


Fig. 7. F-actin controls Yap intracellular dynamics. Representative immunofluorescence with anti-Yap and anti-GFP in 72hpa longitudinal sections of Alpha-Catenin transgenics injected with Jasplakinolide (JASP) and DMSO controls. Yap expression in DMSO (A) and JASP (B) animals. C-D Zoomed areas represented by squares in A-B; single color images showing Yap and DAPI in DMSO (C-C') and JASP (D-D') conditions. Corresponding XZ

projections of distal blastemas C-D highlight intracellular localization (DMSO XZ Distal, JASP XZ Distal). **E** Quantification of Yap intracellular localization by expressing a ratio between average intensities of Nuclear Yap: Cytoplasmic Yap of XZ projections from distal blastemas in DMSO or JASP conditions, at 30 minutes post injection. Higher ratios correspond to higher intensities of nuclear Yap. ***P value<0.001, two tailed, non-parametric Mann-Whitney test. n=8 sections, 4 fish/condition. **F** qPCR determination of *ctgfa* levels in JASP versus DMSO animals, at 30 minutes and 2 hours post injection, time-points when RNA was extracted from blastemas. **P value<0.01; two tailed, non-parametric paired Wilcoxon test, logarithmic scale, base 10. **G-I** Alpha-Catenin expression in DMSO (**G**) and JASP (**I**) animals. **H-J** Zoomed areas represented by squares in G-I, showing Alpha-Catenin in distal blastemas of DMSO (**H**) and JASP (**J**) animals. Corresponding XZ projections of distal blastemas H-J highlight intracellular localization of Alpha-Catenin and DAPI. Intraperitoneal injections were performed in 72hpa animals, 30 minutes pre-fixation of blastemas. n=12 sections, 4 fish/condition. Dashed lines indicate amputation plane. Scale bars=50µm.